Doughnut-shaped soap bubbles

Deison Préve and Alberto Saa[*]

Departamento de Matemática Aplicada, IMECC—UNICAMP, 13083-859 Campinas, São Paulo, Brazil

Soap bubbles are thin liquid films enclosing a fixed volume of air. Since the surface tension is typically assumed to be the only factor responsible for conforming the soap bubble shape, the realized bubble surfaces are always minimal area ones. Here, we consider the problem of finding the axisymmetric minimal area surface enclosing a fixed volume V and with a fixed equatorial perimeter L. It is well known that the sphere is the solution for $V = L^3/6\pi^2$, and this is indeed the case of a free soap bubble, for instance. Surprisingly, we show that for $V < \alpha L^3/6\pi^2$, with $\alpha \approx 0.21$, such a surface cannot be the usual lens-shaped surface formed by the juxtaposition of two spherical caps, but is rather a toroidal surface. Practically, a doughnut-shaped bubble is known to be ultimately unstable and, hence, it will eventually lose its axisymmetry by breaking apart in smaller bubbles. Indisputably, however, the topological transition from spherical to toroidal surfaces is mandatory here for obtaining the global solution for this axisymmetric isoperimetric problem. Our result suggests that deformed bubbles with $V < \alpha L^3/6\pi^2$ cannot be stable and should not exist in foams, for instance.

PACS number(s): 68.15.+e, 47.55.db, 47.55.df

I. INTRODUCTION

Soap bubbles have been attracting the attention of physics and mathematicians for more than two centuries [1]. A soap bubble is a thin liquid film enclosing a given volume of air. Surface tension is usually assumed to be the only factor responsible for conforming the bubble surface shape, and hence the realized surfaces are always minimal area ones. It is well known that the sphere is the solution for one of the most celebrated isoperimetric problems: to find the minimal area surface enclosing a fixed and given volume. Free soap bubbles are known to be spheres.

We consider here the problem of finding the axisymmetric minimal area surface with two simultaneous constraints: a fixed enclosed volume V and a fixed equatorial perimeter L. Since a sphere of radius a is the minimal area surface enclosing a volume $V = 4\pi a^3/3$, it will be also the solution for our problem for this volume and equatorial perimeter $L = 2\pi a$. We are mainly interested in the cases with $L = 2\pi a$ and $V \leqslant 4\pi a^3/3$, for which the solutions may have the shape of a "lens" formed by the juxtaposition of two spherical caps of height $h < a$ [see Fig. 1(a)]. The enclosed volume by these lens-shaped surfaces is

$$V = \frac{\pi h}{3}(3a^2 + h^2), \qquad (1)$$

whereas their surface area is given by

$$A = 2\pi(a^2 + h^2). \qquad (2)$$

As we can see, for a fixed equatorial perimeter $L = 2\pi a$, one can effectively have arbitrarily small enclosed volumes V by choosing arbitrarily small cap heights h since $0 \leqslant V \leqslant L^3/6\pi^2$. On the other hand, the surface area A will be always bounded from below by a positive value, $A > L^2/2\pi$. It is clear that for small cap height h the lens-shaped surface cannot be an efficient surface for enclosing a small volume V with a fixed equatorial perimeter L. Surprisingly, in order to obtain the

global minimum for this axisymmetric isoperimetric problem, a topological transition is mandatory: from the spherical lens-shaped to toroidal surfaces. As we will show, lens-shaped surfaces of equatorial perimeter L are global solutions for our minimal area problem only for volumes V such that

$$\alpha\frac{L^3}{6\pi^2} < V \leqslant \frac{L^3}{6\pi^2}, \qquad (3)$$

with $\alpha \approx 0.21$. For $V < \alpha L^3/6\pi^2$, the axisymmetric minimal area surface enclosing a volume V will be necessarily doughnut shaped as the one depicted in Fig. 1(b), as we will see by considering all solutions of our isoperimetric problem in the following section.

II. THE ISOPERIMETRIC VARIATIONAL PROBLEM

Strictly speaking, the isoperimetric problem, dating from antiquity, concerns finding the plane figure of maximal area with a given perimeter. In a broader sense, however, it includes, for instance, the problem of finding the function $f(x,y)$ which minimizes a given functional

$$S[f] = \iint_{\mathcal{D}} \mathcal{L}(x,y,f,f_x,f_y)\,dxdy, \qquad (4)$$

but subjected to integral constraints of the type

$$\iint_{\mathcal{D}} \mathcal{C}(x,y,f,f_x,f_y)\,dxdy = \text{const}, \qquad (5)$$

where $\mathcal{D}$ is a region of the plane (x,y) and the indices x and y denote the respective partial derivatives. Every function here is assumed to be real and smooth. For our purposes, let us consider the surface (x,y,z) defined by the function $f(x,y) = \pm z$, which we will assume to be non-negative such that $f(x,y) = 0$ for $(x,y) \in \partial\mathcal{D}$.

The standard treatment for the isoperimetric problems involves the associated functional defined as

$$S^*[f] = \iint_{\mathcal{D}} \mathcal{L}^*\,dxdy, \quad \mathcal{L}^* = \mathcal{L} + \lambda\mathcal{C}, \qquad (6)$$
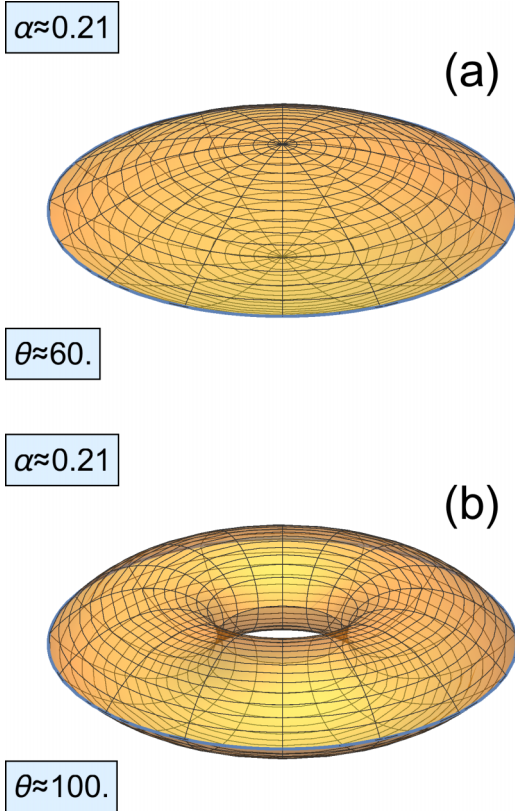
---

[*]Corresponding author: asaa@ime.unicamp.br

FIG. 1. (Color online) Top: Lens-shaped surface of minimal area with perimeter L and volume $V = \alpha L^3/6\pi^2$, with $\alpha \approx 0.21$. No stable lens-shaped surface with $V < \alpha L^3/6\pi^2$ should exist. Bottom: Doughnut-shaped surface of minimal area with perimeter L and $V = \alpha L^3/6\pi^2$. Axisymmetric minimal area surfaces with $V < \alpha L^3/6\pi^2$ are necessarily of this type. No doughnut-shaped minimal area surfaces exist with $V > \alpha L^3/6\pi^2$. In both cases, the angle θ is the internal angle of the surface at the equatorial perimeter.

where λ is a constant (the Lagrange multiplier). The function $f(x,y)$ that extremizes Eq. (4) subjected to the constraint (5) also extremizes the free functional (6), i.e., $f(x,y)$ is a solution of the Euler-Lagrange equations for the associated functional (6). The constant λ is to be determined, among all the integration constants, from the boundary conditions and the integral constraint (5). For the problem of the minimal area axisymmetric surface, one can introduce appropriate polar coordinates (ρ, θ) centered at the surface such that $f = f(\rho)$, leading to the following expression for the area functional:

$$S[f] = 2\pi \int_{\mathcal{D}} \sqrt{1 + f'^2}\, \rho\, d\rho, \tag{7}$$

while the fixed volume constraint will read simply

$$V[f] = 2\pi \int_{\mathcal{D}} f\, \rho\, d\rho = \text{const.} \tag{8}$$

Clearly, the equatorial perimeter will be given by the length of $\partial\mathcal{D}$. In these coordinates, the Euler-Lagrange equation for the associated functional (6) is

$$\frac{1}{\rho} \frac{d}{d\rho}\left(\frac{\rho f'}{\sqrt{1 + f'^2}}\right) = \lambda, \tag{9}$$

which is easily integrated and leads to

$$\frac{\rho f'}{\sqrt{1 + f'^2}} = \frac{\lambda}{2}\rho^2 + C_1. \tag{10}$$

We have two qualitative distinct cases according to the value of C_1. For $C_1 = 0$, we have $f'(0) = 0$, which is indeed a regularity condition for axisymmetric surfaces. However, and more importantly, in this case there is no restriction for the values of ρ and, consequently, $\mathcal{D}$ is a circle. It is quite simple to verify that the solutions of Eq. (10) for this case are the arcs given by

$$[f(\rho) + b]^2 + \rho^2 = r_0^2, \tag{11}$$

with $r_0 = 2/\lambda$ and $r_0 > b \geqslant 0$. These solutions correspond to the usual spherical cap with basis radius $a^2 = r_0^2 - b^2$ and height $h = r_0 - b$. These caps form the lens-shaped solutions for our isoperimetric problem.

Nevertheless, we have also the solutions with $C_1 \neq 0$. Solving Eq. (10) for f' and considering the convenient signs, we have

$$f'(\rho) = \frac{d - x^2}{\sqrt{\left(x^2 - x_{\min}^2\right)\left(x_{\max}^2 - x^2\right)}}, \tag{12}$$

where $x = \lambda\rho$, $d = 2\lambda C_1 > 0$, and

$$x_{\min} = \sqrt{1 + d} - 1, \quad x_{\max} = \sqrt{1 + d} + 1. \tag{13}$$

The first observation here is the most important one: for $C_1 \neq 0$, there will be necessarily restrictions for ρ, and we have indeed $x_{\min} \leqslant \lambda\rho \leqslant x_{\max}$. The region $\mathcal{D}$ is not anymore a circle, but effectively a ring domain. The integral (12) can be solved analytically by using elliptic functions, but for our purposes we opt to solve it numerically. All pertinent details are presented in the Appendix. The second additive integration constant will be chosen in order to have $f(\rho_{\min}) = 0$, with $x_{\min} = \lambda\rho_{\min}$. Notice that $f'(\rho_{\min})$ diverges, assuring in this way that the juxtaposition of the superior and inferior parts of our doughnut-shaped surface will be indeed smooth along the interior radius. An example of solution $f(\rho)$ is depicted in Fig. 2, which corresponds to he doughnut-shaped surface in Fig. 1(b). The equatorial perimeter of the surface will be given by $L = 2\pi\rho_*$, where the radius $\rho_* > \rho_{\min}$ is such that $f(\rho_*) = 0$.

The constant λ can be effectively absorbed by a global rescaling. For each value of $d > 0$, we have a toroidal surface. From Eq. (13), we see that small values of d correspond to the cases with $x_{\min} \approx 0$ and $x_{\max} \approx 2$. These solutions can enclose arbitrarily small volumes, but their area is bounded from below by the area of a lens-shaped solution with the same equatorial perimeter L. On the other hand, the solutions with large d, which corresponds to large $x_{\min}$ and $x_{\max}$, can enclose arbitrarily small volumes with arbitrarily small surface areas. The situation is depicted in the area times volume diagram of Fig. 3. The solid red line corresponds to the doughnut-shaped solutions, while lens-shaped ones correspond to the dashed green line. The doughnut-shaped solution with maximal volume corresponds to the case with $d \approx 1.6235$ [depicted in Figs. 1(b) and 2]. For any other value of d, there are always two minimal area surfaces: one corresponding to small $x_{\min}/x_{\max}$ (small d) and the other to small $(x_{\max} - x_{\min})/x_{\max}$ (large d).
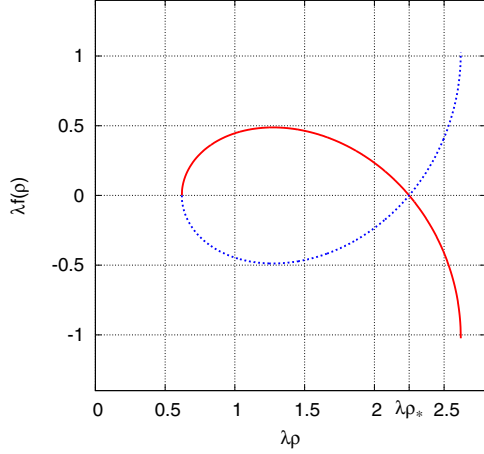
FIG. 2. (Color online) Solid red line: Solution for Eq. (12) with boundary condition $f(\rho_{min}) = 0$ for $d \approx 1.6235$, which corresponds to $\lambda\rho_{min} \approx 0.6197$, $\lambda\rho_* \approx 2.2491$, and $\lambda\rho_{max} \approx 2.6197$. The doughnut-shaped solution depicted in Fig. 1(b) is obtained by the revolution around the vertical axis of the closed curve formed by the solution and its reflection on the horizontal axis (the dashed blue line) for $\rho_{min} \leqslant \rho \leqslant \rho_*$. This particular value of d corresponds to the toroidal solution with maximal enclosed volume. The doughnut-shaped surface is regular everywhere except on the equatorial perimeter $\rho = \rho_*$.

The second one will be the global minimum of the problem (see Fig. 3). We see from the diagram that the lens-shaped surfaces are effectively the only minimal area solution for our problem provided that the condition (3) holds, with $\alpha \approx 0.21$, which corresponds, namely, to the minimal area doughnut-shaped surface of maximum volume. For $V < \alpha L^3/6\pi^2$, we see from the diagram that three minimal area surfaces coexist,
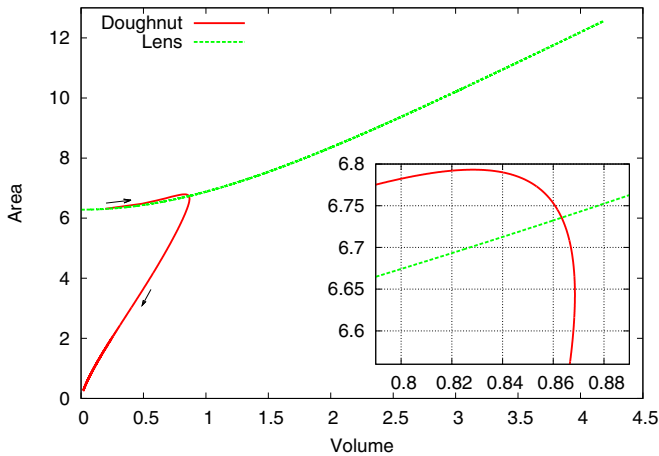

FIG. 3. (Color online) Area times volume diagram for axisymmetric minimal area surface with fixed equatorial perimeter $L = 2\pi$. The solid red line corresponds to the doughnut-shaped solutions, with the arrows indicating the direction of increasing d. The dashed green line corresponds to the lens-shaped solutions. Inset: The region corresponding to the topological transition. The maximum volume for the doughnut-shaped solution is $V \approx 0.869$, corresponding to the case depicted in Fig. 2. An animation illustrating the transition from spherical to toroidal surfaces is available in [2].
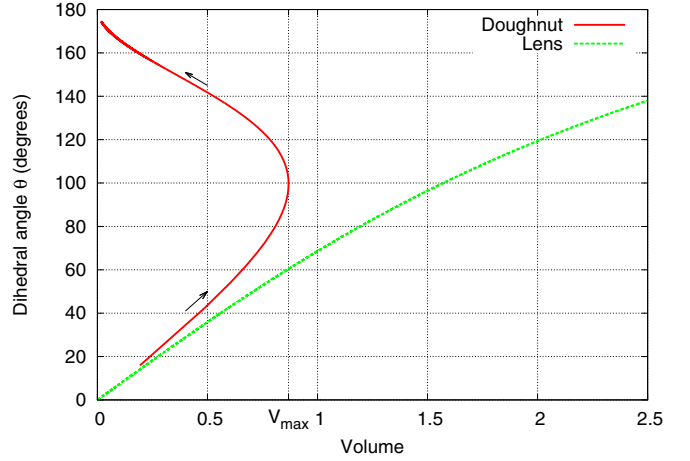

FIG. 4. (Color online) Dihedral angle θ between the tangent planes at the equatorial perimeter as a function of the enclosed volume V for axisymmetric minimal area surfaces with equatorial perimeter $L = 2\pi$. The solid red line corresponds to the doughnut-shaped solutions, with the arrows indicating the direction of increasing d, while the lens-shaped solutions are denoted by the dashed green line. Notice that, for $d \to \infty$, $V \to 0$ and the dihedral angle tends to 180 deg. The doughnut-shaped surface in this limit tends to the usual torus of circular section.

but clearly the global minimum corresponds to the case of doughnut-shaped surfaces with $d > 1.6235$. An animation illustrating the topological transition from spherical to toroidal surfaces according to the value of the ratio V/L^3 is available in [2].

It is interesting to relate the topological transition of the minimal area surfaces to the dihedral angle θ between the tangent planes at the equatorial perimeter. Figure 4 depicts the dependence of θ on the volume V for a fixed equatorial perimeter $L = 2\pi$. For the lens-shaped surfaces, the minimal volume $V = \alpha L^3/6\pi^2$ case corresponds to θ close to 60 deg. This is the case depicted in Fig. 1(a). The doughnut-shapes surface with the same volume has a larger dihedral angle, close to 100 deg [Figs. 1(b) and 2]. Notice that

$$\alpha = 8 - \frac{9}{2}\sqrt{3} = 0.20577\ldots \qquad (14)$$

corresponds to the volume of a lens-shaped surface with dihedral angle $\theta = 60$ deg at the equatorial external perimeter.

Notice that all solutions to our isoperimetrical problem have constant mean curvature and therefore they correspond indeed to pieces of Delaunay surfaces. This can be checked by recalling the first and second, respectively, fundamental forms for our surface of revolution generated by $f(\rho)$: $E = \rho^2$, $F = 0$, $G = 1 + f'^2$; $L = -\rho f'/\sqrt{1 + f'^2}$, $M = 0$, $N = -f''/\sqrt{1 + f'^2}$; and

$$-\frac{1}{\rho}\frac{d}{d\rho}\left(\frac{\rho f'}{\sqrt{1 + f'^2}}\right) = \frac{L}{E} + \frac{N}{G} = 2H, \qquad (15)$$

where H stands for the mean curvature of our surface. Thus, the Euler-Lagrange equation (9) is equivalent to the constraint of constant H. Since H is constant, we can easily evaluate it by taking the point $\bar{\rho}$ such that $f'(\bar{\rho}) = 0$, where $L = 0$ and

$N = -f''(\bar{\rho})$, leading simply to

$$H = -\tfrac{1}{2} f''(\bar{\rho}), \tag{16}$$

which is positive for our toroidal surfaces. The mean curvature can be expressed also as $2H = R_1^{-1} + R_2^{-1}$, where R_1 and R_2 are the radii corresponding to the principal curvatures. The $d \to \infty$ ($V \to 0$) limit of Fig. (4), for which the external dihedral angle tends to 180 deg, is a usual torus of circular section for which $R_1 \ll R_2$, assuring in this way that $2H \approx R_1^{-1} = \text{const}$.

III. FINAL REMARKS

We have shown that the isoperimetric problem of finding an axisymmetric minimal area surface enclosing a fixed volume V and with a fixed equatorial perimeter L exhibits a rather unexpected topological transition in their solutions according to the ratio V/L^3. The typical lens-shaped surfaces formed by two spherical caps are not the global minimum for small enclosed volumes V. The global minimum for the axisymmetric case enclosing small volumes corresponds to toroidal surfaces. The situation considered here resembles in many ways the classical Goldschmidt discontinuous minimal area surface of revolution limited by two coaxial rings separated by a distance ℓ [1,3]. In our case, for V below a critical value, we have two toroidal minimal area surfaces enclosing a given volume. One of them has area smaller than the corresponding lens-shaped surface, while the other has a greater superficial area. In the Goldschmidt case, for ℓ below a certain critical value, we have always two minimal surfaces (catenoids), but only one of them can effectively have a total superficial area smaller than the discontinuous Goldschmidt solution. In fact, the diagram area times ℓ for the catenoids is very similar to our area times volume curve in Fig. 3.

Finally, we cannot ignore that a doughnut-shaped minimal area surface will be ultimately unstable due to phenomena like shrinking [4,5] and Plateau-Rayleigh [6,7] instabilities. This means that, for instance, if one deforms a bubble axisymmetrically in such a way that its equatorial perimeter L is enlarged while its volume V is kept constant, the bubble will be inexorably destroyed when $L^3 > 6\pi^2 V/\alpha$. If a doughnut-shaped bubble is formed, it will probably break apart in smaller daughter bubbles (see, for similar behavior in another context, [8]). It is not difficult to envisage a nonaxisymmetric surface with fixed external perimeter L, enclosing a volume $V < \alpha L^3/6\pi^2$ and with area A smaller than the area of our toroidal surface. Consider, for instance, a sphere with a handle as shown in Fig. 5. The external handle guarantees the constant perimeter constraint. By shrinking its smaller radius, its contribution for the total V and A will be arbitrarily small, and hence they will correspond to the sphere, which is known to be the global solution for the problem and will certainly encapsulate a given volume V with surface area A smaller than our doughnut-shaped surface. This kind of nonaxisymmetric surface might arise from a Plateau-Rayleigh instability, where perturbations with wavelength greater than the smaller dimension of the toroidal surface could grow exponentially until disrupted.

The situation is more intricate, however, if one keeps the perimeter curve fixed, preventing in this way the formulation
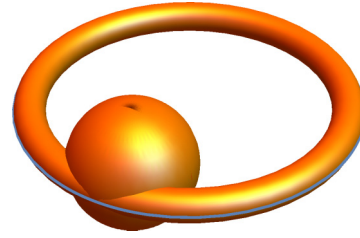

FIG. 5. (Color online) Sphere with a toroidal handle: by shrinking the handle smaller radius, we have a surface with fixed external perimeter L, enclosing a volume $V < \alpha L^3/6\pi^2$, and with area A smaller than our axisymmetric toroidal surface. Axisymmetric surfaces are not global solutions for the problem.

of an axisymmetric problem from the beginning. By similar arguments, we also expect genus 1 minimal area surfaces for small V/L^3 in this case, but the value of the threshold α can be different. Despite being unstable as minimal area surfaces, doughnut-shaped structures are quite common in many dynamical situations, ranging from stains left by a coffee droplet [9] to extracellular polymeric bacterial coverages [10]. In particular, toroidal liquid droplets have been obtained by exploring some pyroelectric effects on wetting processes [11]. We think our result might be useful to shed more light on some of these problems.

APPENDIX: NUMERICS

It is convenient for our purposes to introduce some dimensionless quantities. From Eq. (12), one can introduce the dimensionless function $F(x)$:

$$f(\rho) = \frac{1}{\lambda} F(\lambda\rho), \tag{A1}$$

with

$$F(x) = \int_{x_{\min}}^{x} \frac{d - s^2}{\sqrt{(s^2 - x_{\min}^2)(x_{\max}^2 - s^2)}} \, ds. \tag{A2}$$

It is clear from Eq. (A1) that the constant λ can be absorbed by a global rescaling of the problem. The integral (A2) can be expressed by means of elliptical integrals; see, for instance, formulas (9) and (7) in Secs. 3.152 and 3.153, respectively, of [12]. However, the expressions become rather cumbersome for our manipulations, and we choose to solve Eq. (A2) numerically. The integrand diverges for $x = x_{\min}$ and $x_{\max}$, but the divergence is integrable and it can be easily circumvented, for instance, by introducing the new variable $u^2 = s^2 - x_{\min}^2$. The singularity for $x = x_{\max}$ can be eliminated analogously.

The equatorial perimeter will correspond to the external radius of the doughnut-shaped solution, i.e., to the point $\rho_* = \lambda x_*$ such that $F(x_*) = 0$. The value of x_* can be determined

accurately from Eq. (A1) by using a Newton-Rapson scheme. The equatorial perimeter will be given by

$$L = 2\pi \frac{x_*}{\lambda}. \tag{A3}$$

The volume enclosed by the doughnut-shaped surface will be given by

$$V = \frac{4\pi}{\lambda^3} \int_{x_{\min}}^{x_*} s F(s) \, ds, \tag{A4}$$

and its surface area reads

$$A = \frac{8\pi}{\lambda^2} \int_{x_{\min}}^{x_*} \frac{s^2}{\sqrt{\left(s^2 - x_{\min}^2\right)\left(x_{\max}^2 - s^2\right)}} \, ds. \tag{A5}$$

The area times volume diagram of Eq. (3) is constructed from Eqs. (A4) and (A5) by varying d while keeping L given by Eq. (A3) fixed.

[1] C. Isenberg, *The Science of Soap Films and Soap Bubbles* (Dover, New York, 1992).

[2] See Supplemental Material at http://link.aps.org/supplemental/10.1103/PhysRevE.92.042402 for an animation illustrating the transition from spherical to toroidal surfaces.

[3] H. F. MacNeish, Ann. Math. **7**, 72 (1906); M. E. Sinclair, Ann. Math **9**, 151 (1908).

[4] Z. Yao and M. Bowick, Eur. Phys. J. E **34**, 32 (2011).

[5] E. Pairam and A. Fernández-Nieves, Phys. Rev. Lett. **102**, 234501 (2009).

[6] J. D. McGraw, J. Li, D. L. Tran, A.-C. Shi, and K. Dalnoki-Veress, Soft Matter **6**, 1258 (2010).

[7] H. Mehrabian and J. J. Feng, J. Fluid Mech. **717**, 281 (2013).

[8] J. C. Bird, R. de Ruiter, L. Courbin, and H. A. Stone, Nature (London) **465**, 759 (2010).

[9] A. G. Marin, H. Gelderblom, D. Lohse, and J. H. Snoeijer, Phys. Rev. Lett. **107**, 085502 (2011).

[10] A. Saa and O. Teschke, J. Colloid and Interface Science **304**, 554 (2006).

[11] L. Miccio, M. Paturzo, S. Grilli, V. Vespini, and P. Ferraro, Optics Letters **34**, 1075 (2009).

[12] I. S. Gradshteyn and I. M. Ryzhik, *Table of Integrals, Series, and Products*, 7th ed. (Academic, New York, 2007).